

Influence of SPIO labelling on the function of BMSCs in chemokine receptors expression and chemotaxis

Yuanchun Liu^{Corresp.,1}, Wanyi Huang¹, Huiyang Wang¹, Wei Lu¹, Jiayu Guo¹, Li Yu¹, Lina Wang^{Corresp. 1}

¹ Department of Pediatrics, Guangzhou First People's Hospital, School of Medicine, South China University of Technology, Department of Pediatrics, Guangzhou First People's Hospital, School of Medicine, South China University of Technology, Guangzhou, China

Corresponding Authors: Yuanchun Liu, Lina Wang

Email address: 15372048@qq.com, eywangln@scut.edu.cn

Bone marrow-derived mesenchymal stem cells (BMSCs) are increasingly being used in bone marrow transplantation (BMT) to enable homing of the allogeneic hematopoietic stem cells and suppress acute graft versus host disease (aGVHD). The aim of this study was to optimize the labelling of BMSCs with superparamagnetic iron oxide particles (SPIOs), and evaluate the impact of the SPIOs on the biological characteristics, gene expression profile and chemotaxis function of the BMSCs. The viability and proliferation rates of the SPIO-labeled BMSCs were analyzed by trypan blue staining and CCK-8 assay respectively, and the chemotaxis function was evaluated by the transwell assay. The expression levels of chemokine receptors were measured by RT-PCR and flow cytometry. The SPIOs had no effect on the viability of the BMSCs regardless of the labelling concentration and culture duration. The labelling rate of the cells was higher when cultured for 48h with the SPIOs. Furthermore, cells labeled with 25µg/ml SPIOs for 48h had the highest proliferation rates, along with increased expression of chemokine receptor genes and proteins. However, there was no significant difference between the chemotaxis function of the labeled and unlabeled BMSCs. To summarize, labelling BMSCs with 25µg/ml SPIOs for 48h did not affect their biological characteristics and chemotaxis function, which can be of significance for *in vivo* applications.

1 **Influence of SPIO labelling on the function of BMSCs in chemokine receptors expression**
2 **and chemotaxis**

3 Yuanchun Liu¹, Wanyi Huang¹, Huiyang Wang¹, Wei Lu¹, Jiayu Guo¹, Li Yu¹, Lina Wang¹.

4 Department of Pediatrics, Guangzhou First People's Hospital, School of Medicine, South China
5 University of Technology, No. 1 Panfu Road, Guangzhou 510180, China.

6 Contributions: (I) Conception and design: Yuanchun Liu; (II)Administrative support: Huiyang
7 Wang, Wei Lu; (III)Provision of study materials: Jiayu Guo; (IV)Collection and assembly of
8 data: Wanyi Huang; (V)Data analysis and interpretation: Lina Wang; (VI)Manuscript writing:
9 All authors; Final approval of manuscript: All authors.

10 Correspondence to: Yuanchun Liu, MD, Department of Pediatrics, Guangzhou First People's
11 Hospital, School of Medicine, South China University of Technology, No. 1 Panfu Road,
12 Guangzhou 510180, China. Email: 15372048@qq.com; Li Yu, MD, Department of Pediatrics,
13 Guangzhou First People's Hospital, School of Medicine, South China University of Technology,
14 No. 1 Panfu Road, Guangzhou 510180, China. Email: yuli828@yeah.net; Lina Wang,
15 Department of Pediatrics, Guangzhou First People's Hospital, School of Medicine, South China
16 University of Technology, No. 1 Panfu Road, Guangzhou 510180, China. Email:
17 wanglina_11@yeah.net.

18

19 **Abstract**

20 Bone marrow-derived mesenchymal stem cells (BMSCs) are increasingly being used in bone
21 marrow transplantation (BMT) to enable homing of the allogeneic hematopoietic stem cells and

22 suppress acute graft versus host disease (aGVHD). The aim of this study was to optimize the
23 labelling of BMSCs with superparamagnetic iron oxide particles (SPIOs), and evaluate the
24 impact of the SPIOs on the biological characteristics, gene expression profile and chemotaxis
25 function of the BMSCs. The viability and proliferation rates of the SPIO-labeled BMSCs were
26 analyzed by trypan blue staining and CCK-8 assay respectively, and the chemotaxis function was
27 evaluated by the transwell assay. The expression levels of chemokine receptors were measured
28 by RT-PCR and flow cytometry. The SPIOs had no effect on the viability of the BMSCs
29 regardless of the labelling concentration and culture duration. The labelling rate of the cells was
30 higher when cultured for 48h with the SPIOs. Furthermore, cells labeled with 25µg/ml SPIOs for
31 48h had the highest proliferation rates, along with increased expression of chemokine receptor
32 genes and proteins. However, there was no significant difference between the chemotaxis
33 function of the labeled and unlabeled BMSCs. To summarize, labelling BMSCs with 25µg/ml
34 SPIOs for 48h did not affect their biological characteristics and chemotaxis function, which can
35 be of significance for *in vivo* applications.

36

37 **Key words:** SPIO, mesenchymal stem cell, chemokine receptor, chemotaxis, aGVHD.

38

39 **Introduction**

40 Allogeneic hematopoietic stem cell transplantation (allo-HSCT) is known to improve the
41 outcomes of patients with hematological malignancies ^[1,2]. However, it is beset with several
42 challenges such as the lack of suitable donors ^[3,4] and induction of acute graft versus host disease

43 (aGVHD) [5,6]. Transplantation of *ex vivo*-expanded bone marrow mesenchymal stem cells
44 (BMSCs) [7,8] can obviate the disadvantages of allo-HSCT. BMSCs were first identified by
45 Friedenstein as fibroblast colonies formed by bone marrow explants [9]. Recent studies show that
46 BMSCs can promote the homing of transplanted bone marrow cells through specific chemokines
47 and their receptors, and augment hematopoiesis by secreting multiple cytokines [10-15]. Moreover,
48 the BMSCs have been shown to mitigate severe, steroid-refractory aGVHD in the liver, skin and
49 lungs, although the exact mechanisms are unclear [16-19]. Real-time tracking of the BMSCs after
50 intravenous injection can provide insights into their *in situ* functions. For instance, BMSCs
51 labeled with superparamagnetic iron oxide particles (SPIOs) can be monitored *in vivo* by non-
52 invasive magnetic resonance imaging (MRI). SPIOs have the advantages of non-toxicity,
53 prolonged retention and stable excretion [20-22]. Most studies on labelling BMSCs have been
54 focused on determining the toxicity of the labelling particles and optimizing the concentration
55 for real-time *in vivo* imaging [23-25]. Therefore, little is known regarding the influence of labelling
56 particles on the chemokine gene expression and chemotaxis function of BMSCs, which is critical
57 to their clinical role in allo-HSCT and aGVHD.

58 The aim of our study was to determine the impact of different concentrations and labelling
59 durations of SPIOs on the biological characteristics of the BMSCs. We chose rBMSCs from SD
60 rats for our study, which the physiological characteristics meet the requirements of experimental
61 purposes and the needs of subsequent animal experiments. We found that SPIOs can effectively
62 label rBMSCs without affecting their viability and chemotactic functions. The SPIOs-labeled
63 BMSCs can be used to elucidate the mechanisms underlying their functions in BMT and aGVHD

64 through real-time *in vivo* monitoring.

65

66

67 **Material and methods**

68 **Isolation and culture of rat BMSCs (rBMSCs)**

69 SD male rats aged 4-5 weeks old and weighing about 160-200g obtained from Animal

70 Experiment Center of Southern Medical University were euthanized by intravenous injection and

71 dissected to expose the femur, and the study was approved by the Institutional Animal Care and

72 Use Committee of Guangzhou First People's Hospital. The euthanizing criteria was established

73 according to former experiment. The ends of the femurs were cut with a pair of bone forceps,

74 and the bone marrow was flushed out using a 27-gauge needle attached to a 10 ml syringe

75 containing alpha-DMEM/F12 (1:1) medium. The single cell suspension was seeded in a 25 cm²

76 flask and cultured in alpha-DMEM/F12 supplemented with 10% fetal bovine serum (FBS;

77 Ausgenex, FBS500) and 1% penicillin/streptomycin at 37°C under 5% CO₂ in a humid incubator

78 (Thermo Co.). The culture medium and the non-adherent cells were gently removed 24h later,

79 and fresh medium was added. Thereafter, the cell medium was changed every 2-3 days and the

80 cells were passaged at 90% confluency. The primary isolated rBMSCs were defined as passage

81 0. Cells from passages < 10 were used for the experiments. The methodology is outlined in

82 Figure 1.

83 The rBMSCs were cultured with complete alpha-DMEM/F12 with 0, 25, 50 or 75µg/ml SPIOs

84 for 24, 48 or 72h. The expanded BMSCs were identified by flowcytometry and the labelling rate,

85 proliferation and viability were measured using suitable assays. The expression of different
86 chemokine receptors was analyzed by RT-PCR and flow cytometry. were used to measure the
87 expression of chemokine receptors. Transwell assay was used to evaluate the migration rates of
88 the BMSCs.

89

90 **Flow cytometry**

91 The primary rBMSCs were washed twice with PBS, re-suspended at the density of $1 \times 10^6/\text{ml}$, and
92 incubated with : anti-CD29 (Biolegend Cat # 102221, RRID: AB_528789), anti-CD34 (Santa
93 Cruz Cat # sc-7324, RRID: AB_2291280), anti-CD44 (BD Cat # 553456, RRID: AB_10515282)
94 and anti-CD45 (Biolegend Cat # 202216, RRID: AB_1236411) antibodies at 37°C in the dark for
95 30 min. The stained cells were washed with PBS and re-suspended in $200\mu\text{l}$ PBS($n=3$). The
96 rBMSCs co-cultured with SPIOs for 24h, 48h and 72h were trypsinized and centrifuged at 1500
97 rpm for 15 minutes, and re-suspended in PBS at the density of 1×10^6 cells/tube. The aliquots
98 were incubated with anti-CXCR-4 (Santa Cruz cat. no. sc-53534, RRID: AB_782002), anti-
99 CXCR-7 (R&D Cat # FAB8399RG, RRID: AB_2917964), anti-CCR-10 (R&D Cat #
100 FAB2815A-025, RRID: AB_1151964) and anti-CXCR-3 (R&D Cat # FAB8109P, RRID:
101 AB_2917963) antibodies for 30 minutes at room temperature in the dark. The stained cells were
102 washed and re-suspended in $200\mu\text{l}$ PBS. Unstained controls were also included. The cells were
103 acquired in the BD FACSCANTO Plus 10C flow cytometer (BD Biosciences, Franklin Lakes,
104 NJ, USA) ($n=7$), and the expression of the markers was analyzed by Flowjo software (version
105 Flow Jo X 10.0.7r2; FlowJo LLC, Ashland, OR, USA).

106

107 Cell labelling assay

108 The rBMSCs were cultured till 50% confluent, and incubated with different concentrations (25,
109 50, 75 and 100 μ g/ml) SPIOs (Aladdin, cat. no. I140464) for 24 hours. The medium was
110 discarded and fresh medium lacking SPIOs was added. After culturing for another 24h, 48h and
111 72h, the labeled cells were harvested for subsequent tests(n=3).

112

113 Prussian blue staining

114 The labeled rBMSCs was washed thrice with PBS and fixed with 4% paraformaldehyde for 30
115 minutes. After discarding the paraformaldehyde, the cells were incubated with 2% potassium
116 ferrocyanide in 6% hydrogen acid at room temperature for 30 minutes. The stained cells were
117 washed thrice with Hank's buffer, counterstained with nuclear fast red for 2-5 minutes, and
118 washed again. The number of positively-stained cells were counted under a microscope at 40x
119 magnification, and the percentage of SPIOs-labeled cells to the total number of cells was
120 calculated(n=3).

121

122 Trypan blue staining

123 Labeled rBMSCs were suspended in PBS at the density of 1×10^6 cells/ml, and 90 μ l cell
124 suspension was mixed with 10 μ l 0.4% trypan blue solution. The cells were counted within 3
125 minutes of staining, and the viability was calculated as: number of unstained cells/total
126 cells*100%(n=3).

127

128 CCK-8 assay

129 The rBMSCs were seeded in 96-well plates at the density of 2×10^4 /well and cultured overnight.
130 The medium was discarded the following day, and fresh medium containing different
131 concentrations of SPIOs was added. After culturing for 24h, 48h and 72h, the medium was
132 replaced with 100 μ l fresh medium. CCK-8 reagent was added to each well and the cells were
133 incubated for 2h in the dark. The absorbance (OD) value at 490 nm was measured using a
134 microplate reader (BIO-TEK INSTRUMENTS, INC) (n=5).

135

136 Quantitative reverse transcription-polymerase chain reaction

137 The total RNA was extracted using TRIZOL (Thermo, cat. no. 15596-026) according to the
138 manufacturer's instructions, and reverse transcribed to cDNA using PrimerScript RT Master Mix
139 (Takara, Tokyo, Japan). RT-PCR was performed on the IQ5 System (Bio-Rad) using SYBR
140 Green Mastermix (Takara, Tokyo, Japan) (n=3). Each sample was analyzed in duplicate and the
141 relative expression of the target genes was normalized to beta-actin. The primer sequences are
142 listed in Supplementary Table 1.

143

144 Transwell assay

145 Complete DMEM/F12/F12 (10% FBS) was dispensed into transwell inserts with pore size of
146 8 μ m (Corning cat. no. 3422, Costar, Cambridge, MA, USA) in 24-well plates, and incubated
147 overnight. After discarding the medium, control or SPIO-labeled rBMSCs were seeded into the

148 upper chamber of the inserts in complete medium at the density of 8×10^4 cells/200 μ l, with or
149 without chemokine receptor antagonists TAK799, Maraviroc or LY294002. The lower chambers
150 were filled with medium supplemented with the corresponding chemokines i.e., CXCL-10, CCL-
151 4 and CCL-19. After incubating the cells for 48h, the inserts were removed and the cells
152 remaining on the upper surfaces of the membrane were scraped off. The membranes were then
153 washed twice with PBS, fixed in 4% paraformaldehyde for 10 minutes, and stained with 0.5%
154 crystal violet for 5 minutes. The migrated cells on the lower surface of the membranes were
155 counted in three random fields per well under a microscope at low magnification(n=3).

156

157 **Statistical analysis**

158 Statistical product and service solutions (SPSS) 20.0 software (IBM, Armonk, NY, USA) was
159 used for the statistical analysis. The enumeration data were expressed as mean \pm standard
160 deviation. Multiple groups were compared by one-way analysis of variance (ANOVA) followed
161 by Tukey's post hoc test, or rank sum test followed by Kruskal-Wallis post hoc test. $P < 0.05$ was
162 considered statistically significant.

163

164 **Results**

165 **Isolation and characterization of rBMSCs**

166 The primary rBMSCs were adherent after overnight incubation, and consistently exhibited a
167 uniform fibroblast-like appearance from passage 0 (Figure 2A and B) to passage 10 (Figure 2C
168 and D). As shown in Figure 3, the isolated rBMSCs were CD29+ (96.8%), CD44+ (99.3%),

169 CD34- (99.2%) and CD45- (98.7%). Based on previous reports, our results suggested that the
170 isolated and expanded cells were rBMSCs.

171

172 The BMSCs displayed a fibroblast-like appearance throughout culture. Images show BMSCs
173 from passages (A, C) 0 and (B, D) 10 at 50X and 100X magnification as indicated.

174

175 Flow cytometry plots showing percentages of (A) CD29+, (B) CD44+, (C) CD34- and (D)
176 CD45- cells.

177

178 **rBMSCs were optimally labeled with SPIOs after 48h incubation**

179 The rBMSCs were incubated with different concentrations of SPIOs for varying durations, and
180 the presence of SPIOs was detected by Prussian blue staining. As shown in Figure 4A, cells
181 incubated with SPIOs had dense blue-stained iron particles in their cytoplasm and the intensity of
182 the color deepened with increasing concentrations of SPIOs. In contrast, no blue-stained iron
183 particles were observed in the control group (Figure 4A). Furthermore, the percentage of SPIO-
184 labeled cells increased from 54.67%±1.15% after 24h to 98%±1% after 48h of incubation with
185 50µg/ml SPIOs. The labelling rates of the rBMSCs after 48h incubation with 25, 50 and 75µg/ml
186 SPIOs were 90%±1.73%, 98%±1% and 96%±1% respectively, which were consistently higher
187 than that for the other incubation times. (figure 4B).

188

189 **SPIOs had no detrimental effect on the viability and proliferation of rBMSCs**

190 The possible effect of the SPIOs on the viability of BMSCs was evaluated by trypan blue dye
191 exclusion test. As shown in Figure 4C and D, trypan blue dye exclusion rates differed from
192 $91\% \pm 3.60\%$ to $98.67\% \pm 0.58\%$ across the different concentrations of SPIOs, and were not
193 significantly different between the groups. CCK-8 assay further showed that cells labeled with
194 $25\mu\text{g/ml}$ SPIOs had a higher OD value than the cells incubated with higher doses of SPIOs. In
195 addition, the OD values of cells incubated with SPIOs for 24h and 72h showed no significant
196 difference for the different concentrations (Figure 4E).

197

198 (A) Representative images showing Prussian blue-stained iron particles in the BMSCs labeled
199 with different concentrations of SPIOs for varying durations. (B) Labelling rate in the indicated
200 groups. (C) Representative images showing live cells in the indicated groups after trypan blue
201 staining. (D) Viability rates in the indicated groups. (E) Proliferation rates in the indicated groups
202 as measured by CCK-8 test. Data are individual means or the mean \pm SD of each group from
203 three separate experiments. * $p < 0.05$, ** $p < 0.01$, *** $p < 0.001$

204

205 **SPIOs-labeled rBMSCs expressed higher levels of chemokine receptors and cytokines**

206 As shown in Figure 5A, the control and $25\mu\text{g/ml}$ SPIOs-labelled cells expressed consistently
207 high levels of CCR5, CCR10, CXCR3, CXCR5 and IL11 mRNAs after 48h of incubation.
208 Furthermore, cells incubated with $25\mu\text{g/ml}$ SPIOs for 48h showed significant upregulation of
209 CCR5 and CXCR5 compared to the 72h group for the same concentration ($p < 0.05$), and of
210 CCR10 and CXCR3 compared to cell incubated with $50\mu\text{g/ml}$ SPIOs for 24h. Likewise, IL-6

211 and CXCR7 genes were also upregulated in the 25 μ g/ml SPIOs/48h group compared to the
212 control and 25 μ g/ml SPIOs/24h group, and IL-11 was upregulated compared to that in the
213 50 μ g/ml SPIOs/48h group (Figure 5B).

214 Furthermore, flow cytometry experiments showed that the percentage of CXCR3⁺ cells in the
215 rBMSCs treated with 25 μ g/ml SPIOs for 24, 48 and 75h were 26.58% \pm 3.68%, 71.02% \pm 9.93 and
216 58.31% \pm 13.09% respectively, and that of CCR10⁺ cells at the respective time points were
217 25.43% \pm 9.49%, 43.09% \pm 6.68 and 20.72% \pm 1.89%. The untreated control cells also showed a
218 higher expression of CXCR3 after 48h, whereas the percentage of CCR10⁺ cells was unaffected
219 by the duration of culture. There was no significant difference in the percentage of CXCR3⁺ or
220 CCR10⁺ cells between the control and 25 μ g/ml SPIOs/48h groups (Figure 6A-C). The
221 percentage of CXCR7⁺ cells in the control group after 24, 48 and 72h of culture were
222 67.79% \pm 7.77%, 68.59% \pm 6.91 and 53.02% \pm 8.82% respectively, which were significantly higher
223 than in the 25 μ g/ml SPIOs-labeled group at each time point (p <0.001; Figure 5E). Nevertheless,
224 rBMSCs labeled with 25 μ g/ml SPIOs for 48h had the highest percentage of CXCR7⁺ cells
225 (30.03% \pm 9.38%) compared to those labeled with higher concentrations of SPIOs for the same
226 duration. No significant difference was observed between the different SPIO-labeled groups
227 incubated for 24h or 72h.

228 The expression level of CXCR4 was the highest amongst all chemokine receptors in both the
229 control and SPIOs-labeled groups. The percentage of CXCR4⁺ cells in the control and 25 μ g/ml
230 SPIOs-labeled groups were 94.81% \pm 1.72% and 93.47% \pm 3.41% respectively after 24h of culture,
231 and were higher than that in the 50/75 μ g/ml SPIOs-labeled groups for the same duration

232 (p<0.001). In contrast, the cells incubated with 25µg/ml SPIOs for 48h or 72h had a higher
233 proportion of CXCR4+ cells compared to the control (p<0.01 at 48h) and other labeled groups
234 (p<0.05 vs 75µg/ml SPIOs-labeled group at 72h).

235

236 **SPIOs did not affect the migration and chemotactic function of rBMSCs**

237 To determine the effect of the SPIOs on the chemotactic migration of rBMSCs *in vitro*, we
238 cultured the control or 25µg/ml SPIOs-labeled cells in a transwell system in the presence or
239 absence of the CXCL10 (TAK 799), CCL4 (MARAVIORIC) and CCL19 (LY294002)
240 antagonists, and added the respective chemokines to the lower chambers (Figure 7A). After 48
241 hours, the number of BMSCs that had migrated to the other side of the transwell membrane was
242 counted in each group. The migration rates of both the control and SPIOs-labeled cells were
243 significantly higher in the absence of the chemokine antagonists (p<0.001). The percentage of
244 migrating cells per field in response to CXCL10, CCL4 and CCL19 were 81.67±7.36%,
245 82.00±6% and 69.33±3.05% respectively in the control group, and 74.67±2.51%, 82±2% and
246 /68.33±1.52% in the SPIOs-labeled group. The migration rates of the control group decreased to
247 29.33±4.04%, 18.00±3% and 20.00±4% in the presence of TAK 799, MARAVIORIC and
248 LY294002 respectively, and that of the SPIOs-labeled cells decreased to 32.33±2.08%,
249 27.33±2.51% and 29.67±2.08% (Figure 7B). There was no significant difference in the migration
250 rates of the control and SPIOs-labeled BMSCs in any of the conditions, indicating that the SPIOs
251 had no effect on the migration and chemotactic behavior of the rBMSCs.

252

253 Discussion

254 We found that labelling rBMSCs with SPIOs did not affect their viability or chemotactic
255 functions. The cells were optimally labeled when incubated with 25µg/ml SPIOs for 48h, which
256 increased the expression levels of chemokines and chemokine receptors, and therefore
257 maintained their chemotactic migration *in vitro*.

258 A previous study showed that labelling BMSCs with ferucarbotran, a contrast agent consisting of
259 iron oxide microparticles, decreased their migration ability in a dose-dependent manner [11]. We
260 labeled the rBMSCs with a lower concentration of SPIOs to achieve an efficient labelling rate
261 without compromising on cell viability. This is the first study to show that BMSCs incubated
262 with 25µg/ml SPIOs for 48h can be effectively labeled, while maintaining viability and
263 migration ability. This finding is of clinical significance since SPIOs-labeled BMSCs can be
264 tracked *in vivo* to determine their role in the homing of allo-hematopoietic stem cells and the
265 mitigation of aGVHD. The latter is the main life-threatening complication of allo-HSCT. Several
266 clinical and animal model studies have shown that transplantation of BMSCs improve the
267 outcomes of allo-HSCT [5,26,27]. Cynthia et al conducted a meta-analysis and found that
268 allogeneic BMSCs can be used for the prophylaxis and treatment of aGVHD [28]. Therefore, our
269 results can be helpful in elucidating the mechanisms underlying the clinical benefits of BMSCs.

270 The SPIOs-labeled BMSCs expressed higher levels of different chemokines compared to the
271 unlabeled controls. While CXCR4 mRNA was upregulated in the labeled cells, the percentage of
272 cells expressing CXCR4 protein were similar across all groups. This can be attributed to the fact
273 that gene expression is regulated at the transcriptional, mRNA processing and translational

274 levels, any of which may influence the surface expression of the protein. In addition, the cells
275 labeled with 25ug/ml SPIOs for 48h showed the highest expression of CXCR7 among all groups.
276 However, there was no significant difference between the migration rates of the labeled and
277 unlabeled BMSCs, which suggests that the chemokine receptors affect the migration of BMSCs
278 by varying degrees. Given the higher expression of CXCR4 in the SPIOs-labeled cells compared
279 to the controls, we surmise that it may be an important factor in the chemotactic migration of
280 BMSCs.

281 Interestingly, the labelling rate was higher in cells incubated with the SPIOs for 48h compared to
282 24h or 72h. This is likely due to the fact that the number of cells accelerated rapidly during
283 prolonged culture while the amount of SPIOs remained the same. The labeled cells may allocate
284 the SPIOs into their descendant cells for several generations but after a certain threshold, the
285 amount of SPIOs dilutes away. Thus, the number of labeled cells initially increased in a time-
286 dependent manner before decreasing.

287 There are several limitations in our study that ought to be considered. First, we did not analyze
288 the secreted cytokine profile of the labeled BMSCs, which is of clinical relevance the cytokines
289 secreted by the BMSCs influence hematopoiesis. Therefore, our next objective will be to analyze
290 the mRNA and protein levels of multiple cytokines in the labeled BMSCs. Furthermore, other
291 genes involved in BMSC migration will also have to be analyzed. Finally, the clinical
292 applicability of the SPIOs-labeled BMSCs will have to be validated in an in vivo aGVHD model.
293 To summarize, our findings will help facilitate greater clinical use of Fe nanoparticles.

294

295 **Conclusions**

296 We have demonstrated for the first time that SPIOs can effectively label rBMSCs without
297 affecting their viability and chemotactic functions. Thus, SPIOs-labeled BMSCs can be used to
298 elucidate the mechanisms underlying their functions in BMT and aGVHD through real-time *in*
299 *vivo* monitoring.

300

301 **Acknowledgment:** During the whole research, colleagues from the laboratory of Pediatrics and
302 Gastroenterology of Guangzhou First People's Hospital gave great support. Here we would like
303 to thank their efforts.

304

305 **Ethical Statement:** The procedure for extracting primary cells from animals was reviewed and
306 approved by the Review Opinions of Laboratory Animal Ethics Committee of Guangdong
307 Pharmaceutical University.

308

309 **Data assess statement:** The data that support the findings of this study are available upon
310 reasonable request from the authors.

311 **Conflict of Interest:** All authors have completed the ICMJE uniform disclosure form . The
312 authors have no conflicts of interest to declare.

313 **Open Access Statement:** This is an Open Access article distributed in accordance with the
314 Creative Commons Attribution-NonCommercial-NoDerivs 4.0 International License (CC BY-
315 NC-ND 4.0), which permits the non-commercial replication and distribution of the article with

316 the strict proviso that no changes or edits are made and the original work is properly cited
317 (including links to both the formal publication through the relevant DOI and the license). See:
318 <https://creativecommons.org/licenses/by-nc-nd/4.0/>.

319 **Fundings:** This work was Funding by Science and Technology Projects in Guangzhou. The item
320 number is : 202102080130.

321

322 **References**

- 323 1. Better leukemia-free and overall survival in AML in first remission following
324 cyclophosphamide in combination with busulfan compared with TBI. Copelan EA, Hamilton
325 BK, Avalos B, Ahn KW, Bolwell BJ, Zhu X, Aljurf M, van Besien K, Bredeson C, Cahn JY,
326 Costa LJ, de Lima M, Gale RP, Hale GA, Halter J, Hamadani M, Inamoto Y, Kamble RT,
327 Litzow MR, Loren AW, Marks DI, Olavarria E, Roy V, Sabloff M, Savani BN, Seftel M,
328 Schouten HC, Ustun C, Waller EK, Weisdorf DJ, Wirk B, Horowitz MM, Arora M, Szer J,
329 Cortes J, Kalaycio ME, Maziarz RT, Saber W. *Blood*. 2013 Dec 5;122(24):3863-70. doi:
330 10.1182/blood-2013-07-514448. Epub 2013 Sep 24. PMID: 24065243; PMCID:
331 PMC3854108.
- 332 2. Hematopoietic Stem Cell Transplantation in Pediatric Acute Lymphoblastic Leukemia. Pietro
333 Merli, Mattia Algeri, Francesca Del Bufalo, Franco Locatelli. *Current Hematologic*
334 *Malignancy Reports*, 14, 94-105(2019).
- 335 3. A Review of Myeloablative vs Reduced Intensity/Non-Myeloablative Regimens in
336 Allogeneic Hematopoietic Stem Cell Transplantations. Erden Atilla, Pınar Ataca Atilla, and
337 Taner Demirer. *Balkan Med J*. 2017 Jan; 34(1): 1–9.
- 338 4. Effects of post-remission chemotherapy before allo-HSCT for acute myeloid leukemia during
339 first complete remission: a meta-analysis. Yangmin Zhu, Qingyan Gao, Jun Du, Jing Hu, Xu
340 Liu, Fengkui Zhang. *Annals of Hematology* volume 97, pages1519–1526 (2018).
- 341 5. Acute Graft-Versus-Host Disease: A Brief Review. Elifcan Aladağ, Engin Kelkitli, Hakan

- 342 Göker. Turkish Journal of Hematology. 2020 Mar; 37(1): 1–4.
- 343 6. Current Preventions and Treatments of aGVHD: From Pharmacological Prophylaxis to
344 Innovative Therapies. Sina Naserian, Mathieu Leclerc, Sara Shamdani ,Georges Uzan.
345 Frontiers in Immunol. 2020 Dec 17;11:607030. doi: 10.3389/fimmu.2020.607030.
346 eCollection 2020.
- 347 7. Mesenchymal Stromal Cells As Prophylaxis For Graft-Versus-Host Disease In Haplo-
348 Identical Hematopoietic Stem Cell Transplantation Recipients With Severe Aplastic Anemia
349 - A systematic Review and Meta-Analysis. Ruonan Li, Jingke Tu, Jingyu Zhao, Hong Pan,
350 Liwei Fang and Jun Shi. Stem cell research and therapy, (2021)12:106.
- 351 8. Mesenchymal Stem Cell Therapy Overcomes Steroid Resistance In Severe Gastrointestinal
352 Acute Graft-Versus-Host Disease. Kyoko Moritani, Reiji Miyawaki, Kiriko Tokuda,
353 Fumihiko Ochi , Minenori Eguchi-Ishimae , Hisamichi Tauchi, Mariko Eguchi, Eiichi Ishii,
354 Kozo Nagai. Case Reports in Transplantation, Volume 2019, Article ID 7890673, 5 pages
355 <https://doi.org/10.1155/2019/789067>
- 356 9. Bone marrow osteogenic stem cells: in vitro cultivation and transplantation in diffusion
357 chambers. Friedenstein AJ, Chailakhyan RK, Gerasimov UV. Cell Tissue Kinet. 1987
358 May;20(3):263-72. doi: 10.1111/j.1365-2184.1987.tb01309.x. PMID: 3690622.
- 359 10. Modelling of the SDF-1/CXCR4 Regulated in vivo Homing of Therapeutic Mesenchymal
360 stem/stromal Cells in Mice. Wang Jin, Xiaowen Liang, Anastasia Brooks, Kathryn Futrega,
361 Xin Liu, Michael R. Doran, Matthew J. Simpson, Michael S. Roberts, Haolu Wang. PeerJ,
362 2018,6(6);6072.
- 363 11. Augmented Migration of Mesenchymal Stem Cells Correlates With the Subsidiary CXCR4
364 Variant. Asieh Heirani-Tabasi, Hojjat Naderi-Meshkin, Maryam M. Matin, Mahdi
365 Mirahmadi, Mina Shahriyari, Naghmeh Ahmadiankia, Nasser Sanjar Moussavi, Hamid Reza
366 Bidkhorji, Mahmood Raeesolmohaddeseen, Ahmad Reza Bahrami. Cell Adhesion &
367 Migration. 2018, VOL. 12, NO. 2, 118–126.
- 368 12. The Role of Chemokines in Mesenchymal Stem Cell Homing to Wounds. Anne M. Hocking,

- 369 Advances in wound care, volume 4, November 11.
- 370 13. Mild hypoxia and human bone marrow mesenchymal stem cells synergistically enhance
371 expansion and homing capacity of human cord blood CD34+ stem cells. Fatemeh
372 Mohammadali, Saeid Abroun, Amir Atashi. Iranian Journal of Basic Medical Sciences,
373 2018,21(7):709-716;.
- 374 14. Optimization of Adipose Tissue-Derived Mesenchymal Stem Cells by Rapamycin in a
375 Murine Model of Acute Graft-Versus-Host Disease. Kim KW, Moon SJ, Park MJ, Kim BM,
376 Kim EK, Lee SH, Lee EJ, Chung BH, Yang CW, Cho ML. Stem Cell Res Ther. 2015 Oct
377 23;6:202. doi: 10.1186/s13287-015-0197-8. Erratum in: Stem Cell Res Ther. 2016;7(1):80.
378 PMID: 26497134; PMCID: PMC4619057.
- 379 15. Human Bone Marrow Mesenchymal Stem Cells Secrete Endocannabinoids That Stimulate in
380 Vitro Hematopoietic Stem Cell Migration Effectively Comparable to Beta-Adrenergic
381 Stimulation. Köse S, Aerts-Kaya F, Köprü ÇZ, Nemutlu E, Kuşkonmaz B, Karaosmanoğlu
382 B, Taşkiran EZ, Altun B, Uçkan Çetinkaya D, Korkusuz P. Experimental Hematology. 2018
383 Jan;57:30-41.e1. doi: 10.1016/j.exphem.2017.09.009. Epub 2017 Oct 10. PMID: 29030083.
- 384 16. Mouse Bone Marrow-Derived Mesenchymal Stem Cells Inhibit leukemia/lymphoma Cell
385 Proliferation in Vitro and in a Mouse Model of Allogeneic Bone Marrow Transplant. Song
386 N, Gao L, Qiu H, Huang C, Cheng H, Zhou H, Lv S, Chen L, Wang J. International Journal
387 of Molecular Medicine, 36: 139-149, 2015.
- 388 17. Adoptive Transfer of Treg Cells Combined With Mesenchymal Stem Cells Facilitates
389 Repopulation of Endogenous Treg Cells in a Murine Acute GVHD model. Eun-Sol Lee,
390 Jung-Yeon Lim, Keon-Il Im, Nayoun Kim, Young0Sun Nam, Young-Woo Jeon, Seok-Goo
391 Cho. PLOS ONE, 2015; 10(9): e0138846.
- 392 18. Human mesenchymal stromal cells attenuate graft-versus-host disease and maintain graft-
393 versus-leukemia activity following experimental allogeneic bone marrow transplantation.
394 Auletta JJ, Eid SK, Wuttisarnwattana P, Silva I, Metheny L, Keller MD, Guardia-Wolff R,
395 Liu C, Wang F, Bowen T, Lee Z, Solchaga LA, Ganguly S, Tyler M, Wilson DL, Cooke KR.

- 396 Stem Cells. 2015 Feb;33(2):601-14. doi: 10.1002/stem.1867. PMID: 25336340; PMCID:
397 PMC4304927.
- 398 19. Children and Adults with Refractory Acute Graft-versus-Host Disease Respond to Treatment
399 with the Mesenchymal Stromal Cell Preparation “MSC-FFM”—Outcome Report of 92
400 Patients. Bonig H, Kuçi Z, Kuçi S, Bakhtiar S, Basu O, Bug G, Dennis M, Greil J, Barta A,
401 Kállay KM, Lang P, Lucchini G, Pol R, Schulz A, Sykora KW, Teichert von Luettichau I,
402 Herter-Sprie G, Ashab Uddin M, Jenkin P, Alsultan A, Buechner J, Stein J, Kelemen A,
403 Jarisch A, Soerensen J, Salzmann-Manrique E, Hutter M, Schäfer R, Seifried E, Paneesha S,
404 Novitzky-Basso I, Gefen A, Nevo N, Beutel G, Schlegel PG, Klingebiel T, Bader P. Cells.
405 2019 Dec 5;8(12):1577. doi: 10.3390/cells8121577. PMID: 31817480; PMCID:
406 PMC6952775.
- 407 20. Viability and MR Detectability of Iron Labeled Mesenchymal Stem Cells Used for
408 Endoscopic Injection Into the Porcine Urethral Sphincter. Will S, Martirosian P, Eibofner F,
409 Schick F, Bantleon R, Vaegler M, Grözinger G, Claussen CD, Kramer U, Schmehl J. NMR
410 in Biomedicine, 2015, 28(8):1049-58.
- 411 21. Tracking Mesenchymal Stem Cells Using Magnetic Resonance Imaging. Rosenberg JT,
412 Yuan X, Grant S, Ma T. Brain Circulation. 2016 Jul-Sep;2(3):108-113. doi: 10.4103/2394-
413 8108.192521. Epub 2016 Oct 18. PMID: 30276283; PMCID: PMC6126273.
- 414 22. Effects of Labelling Human Mesenchymal Stem Cells With Superparamagnetic Iron Oxides
415 on Cellular Functions and Magnetic Resonance Contrast in Hypoxic Environments and
416 Long-Term Monitoring. Rosenberg JT, Yuan X, Helsper SN, Bagdasarian FA, Ma T, Grant
417 SC. Brain Circulation, 2018 Jul-Sep;4(3):133-138. doi: 10.4103/bc.bc_18_18. Epub 2018
418 Oct 9. PMID: 30450421; PMCID: PMC6187941.
- 419 23. A New Method for Preparing Mesenchymal Stem Cells and Labelling With Ferumoxytol for
420 Cell Tracking by MRI. Liu L, Tseng L, Ye Q, Wu YL, Bain DJ, Ho C. Scientific Reports.
421 2016 May 18;6:26271. doi: 10.1038/srep26271. PMID: 27188664; PMCID: PMC4870722.
- 422 24. Magnetic resonance contrast and biological effects of intracellular superparamagnetic iron

- 423 oxides on human mesenchymal stem cells with long-term culture and hypoxic exposure.
424 Rosenberg JT, Sellgren KL, Sachi-Kocher A, Calixto Bejarano F, Baird MA, Davidson MW,
425 Ma T, Grant SC. *Cytotherapy*. 2013 Mar;15(3):307-22. doi: 10.1016/j.jcyt.2012.10.013.
426 Epub 2012 Dec 17. PMID: 23253438.
- 427 25. Dose-response of superparamagnetic iron oxide labelling on mesenchymal stem cells
428 chondrogenic differentiation: a multi-scale in vitro study. Roeder E, Henrionnet C, Goebel
429 JC, Gambier N, Beuf O, Grenier D, Chen B, Vuissoz PA, Gillet P, Pinzano A. *PLoS One*.
430 2014 May 30;9(5):e98451. doi: 10.1371/journal.pone.0098451. PMID: 24878844; PMCID:
431 PMC4039474.
- 432 26. Physical function and quality of life in patients with chronic GvHD: a summary of preclinical
433 and clinical studies and a call for exercise intervention trials in patients. Fiuza-Luces C,
434 Simpson RJ, Ramírez M, Lucia A, Berger NA. *Bone Marrow Transplant*. 2016 Jan;51(1):13-
435 26. doi: 10.1038/bmt.2015.195. Epub 2015 Sep 14. PMID: 26367233; PMCID:
436 PMC4703521.
- 437 27. Mouse Bone Marrow-Derived Mesenchymal Stem Cells Inhibit leukemia/lymphoma Cell
438 Proliferation in Vitro and in a Mouse Model of Allogeneic Bone Marrow Transplant. Song
439 N, Gao L, Qiu H, Huang C, Cheng H, Zhou H, Lv S, Chen L, Wang J. *International journal*
440 *of molecular medicine*. 2015 Jul;36(1):139-49. doi: 10.3892/ijmm.2015.2191. Epub 2015
441 Apr 21. PMID: 25901937; PMCID: PMC4494598.
- 442 28. Mesenchymal stromal cells for the prophylaxis and treatment of graft-versus-host disease-a
443 meta-analysis. Morata-Tarifa C, Macías-Sánchez MDM, Gutiérrez-Pizarraya A, Sanchez-
444 Pernaute R. *Stem Cell Research & Therapy*. 2020 Feb 18;11(1):64. doi: 10.1186/s13287-
445 020-01592-z. PMID: 32070420; PMCID: PMC7027118.

Figure 1

Schematics of the experimental design.

The rBMSCs were cultured with complete alpha-DMEM/F12 with 0, 25, 50 or 75 μ g/ml SPIOs for 24, 48 or 72h. The expanded BMSCs were identified by flowcytometry and the labelling rate, proliferation and viability were measured using suitable assays. The expression of different chemokine receptors was analyzed by RT-PCR and flow cytometry. were used to measure the expression of chemokine receptors. Transwell assay was used to evaluate the migration rates of the BMSCs.

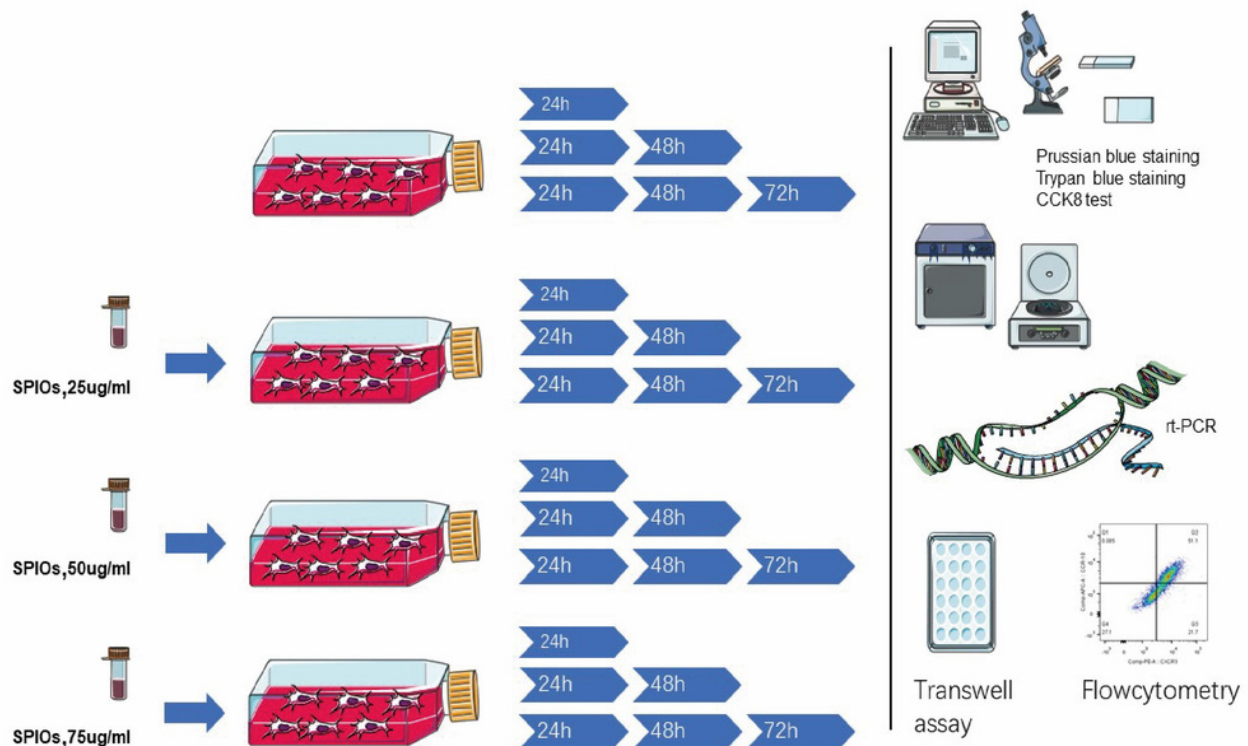


Table 1 (on next page)

This is the primier sequences of RT-PCR testing.

The primier sequences of RT-PCR testing.

Table 1. Primer sequences for reverse transcription-quantitative polymerase chain reaction analysis.

Gene	Forward(5'-3')	Reverse(5'-3')
CXCR4	TGCCATGGAAATATACTTCGG	TGCCCACTATGCCAGTCAAG
CCR10	GGTGGCTGTGCTGGGTTTGG	GGAGGTGGGAGATCGGGTAGTTC
CXCR3	GCCAGTCCTCTACAGCCTCCTC	ACAGCCAGGTGGAGCAGGAAG
CXCR5	GAACTCCCCGATATCGCTAGAC	TGGCCAGTTCCTTGTACAGAT
CXCR7	CCGCGAGGTCACCTTGGTT	CAGTGTGTGTCGTAGCCTGT
IL-6	GCCCACCAGGAACGAAAGTC	TGGCTGGAAGTCTCTTGCGG
IL-11	CTTCAGACCCTCGTGCAGAT	CAGGAAGCTGCAAAGATCCCA

CXCR4, CXC-chemokine receptor CXCR4; CCR10, CC chemokine receptor CCR10; CXCR3, CXC-chemokine receptor CXCR3; CXCR5, CXC-chemokine receptor CXCR5; CXCR7, CXC-chemokine receptor CXCR7; IL-6, interleukin-6; IL-11, interleukin-11.

Figure 2

The morphology of the BMSCs.

The BMSCs displayed a fibroblast-like appearance throughout culture. Images show BMSCs from passages (A, C) 0 and (B, D) 10 at 50X and 100X magnification as indicated.

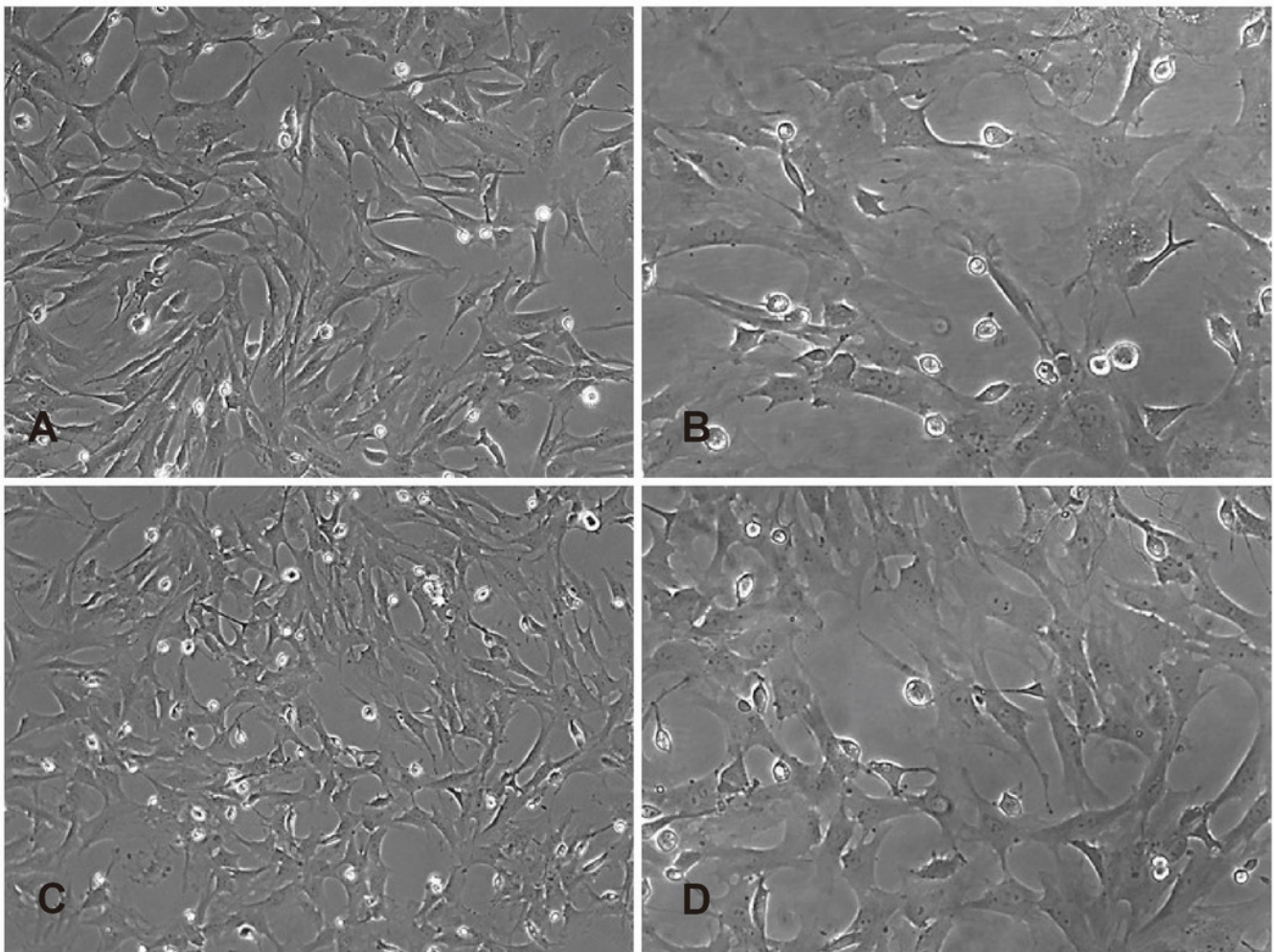
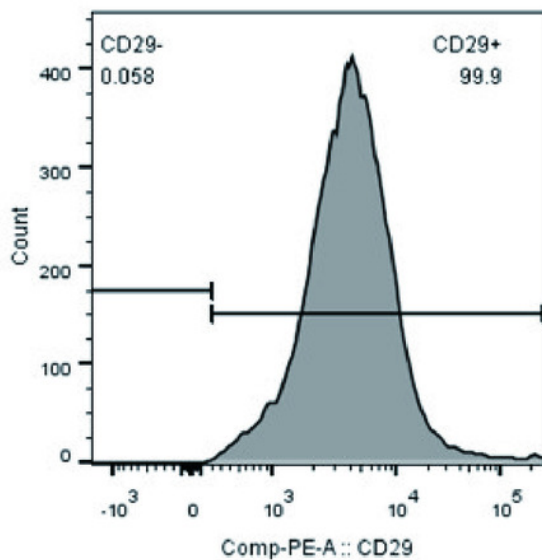


Figure 3

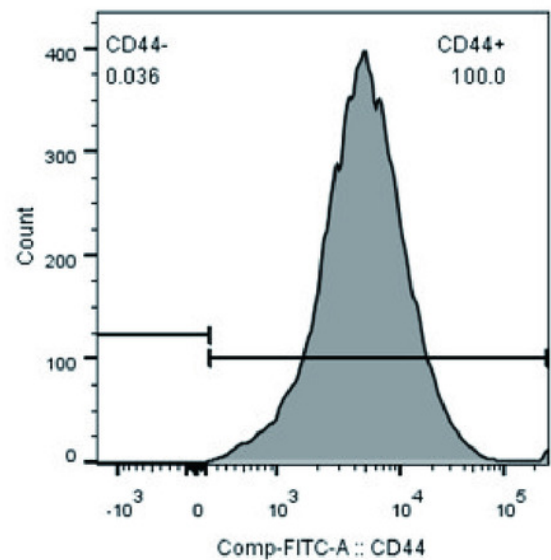
Identification of BMSCs.

Flow cytometry plots showing percentages of (A) CD29+, (B) CD44+, (C) CD34- and (D) CD45- cells.

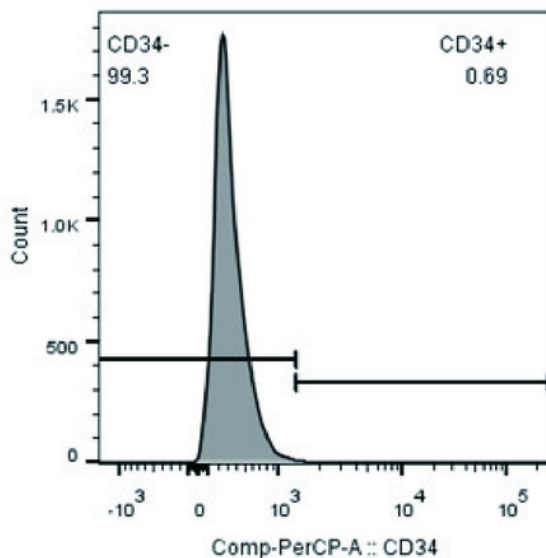
A



B



C



D

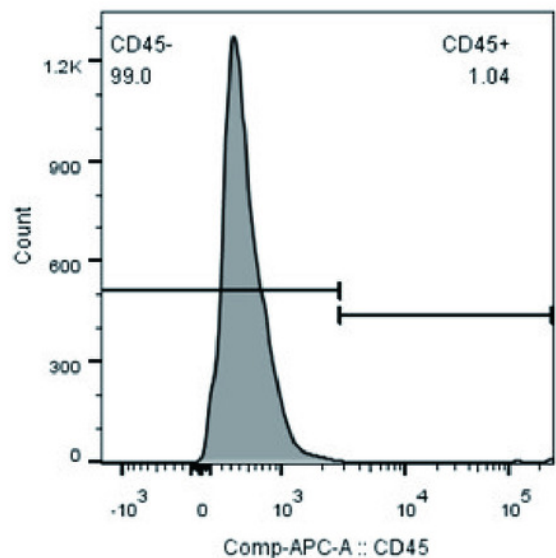


Figure 4

Labelling rate of BMSCs.

(A) Representative images showing Prussian blue-stained iron particles in the BMSCs labeled with different concentrations of SPIOs for varying durations. (B) Labelling rate in the indicated groups. (C) Representative images showing live cells in the indicated groups after trypan blue staining. (D) Viability rates in the indicated groups. (E) Proliferation rates in the indicated groups as measured by CCK-8 test. Data are individual means or the mean \pm SD of each group from three separate experiments. * $p < 0.05$, ** $p < 0.01$, *** $p < 0.001$

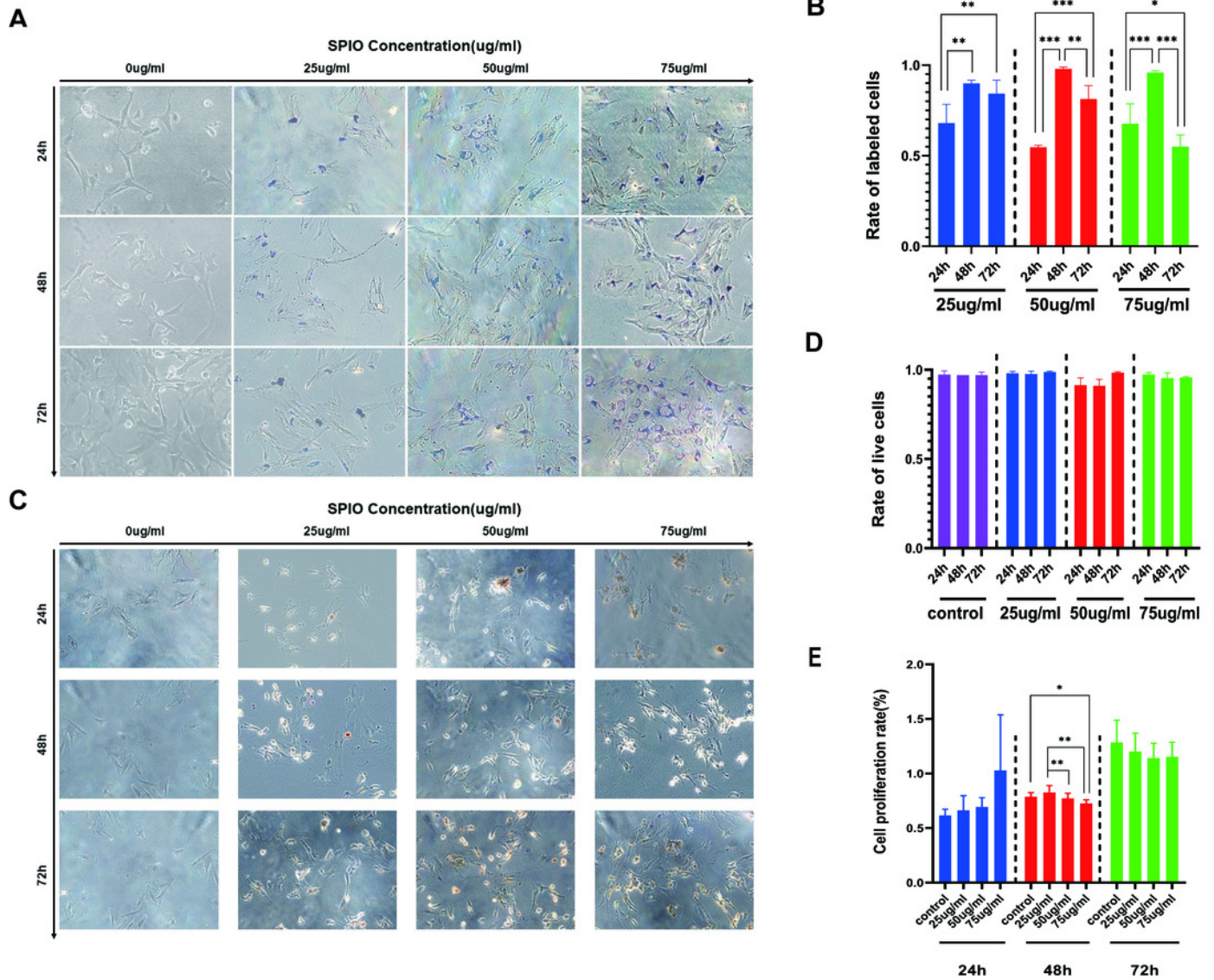


Figure 5

SPIO labelling upregulated chemokine receptor and cytokine genes in BMSCs.

(A, B) The expression level of CCR5, CCR10, CXCR3, CXCR5, IL11, IL 6 and CXCR7 in in the indicated groups. Different colors correspond to the labelling concentrations (25/50/75 μ g/ml) and culture durations (24/48/72h). Data are individual means or the mean \pm SD of each group from three separate experiments. * p <0.05, ** p <0.01, *** p <0.001

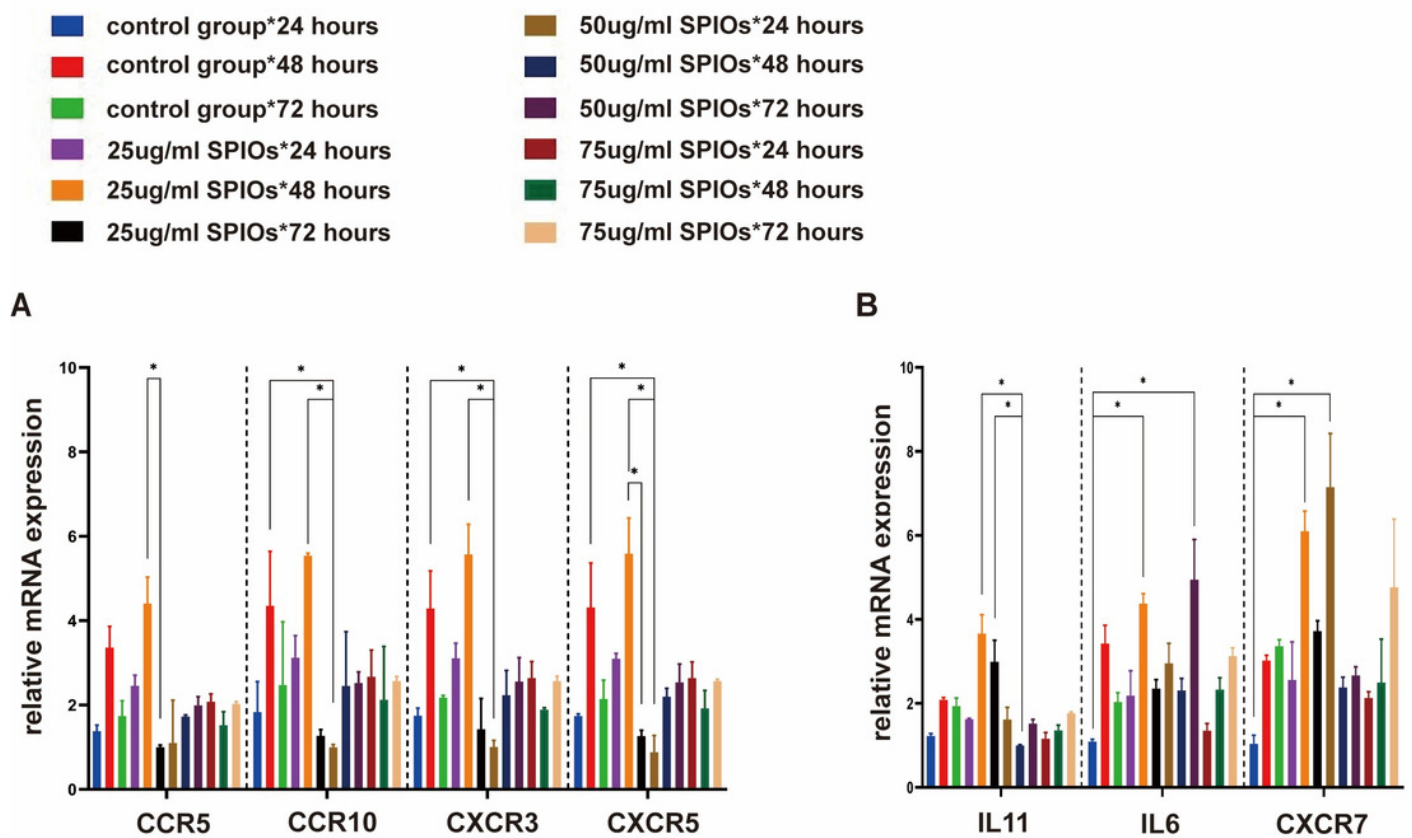


Figure 6

SPIO labelling increased percentage of BMSCs expressing chemokine receptors.

(A) Flow cytometry plots showing percentage of CXCR3/CCR10 control and SPIOs-labeled BMSCs. (D) Flow cytometry plots showing percentage of CXCR7/CXCR4 control and labeled BMSCs. Different colors of the bars on top right correspond to the labelling concentrations of SPIOs. (B) CXCR3 expression in different groups. (C) CCR10 expression in different groups. (E) CXCR7 expression in different groups. (F) CXCR4 expression in different groups. Data are individual means or the mean \pm SD of each group from three separate experiments.

* $p < 0.05$, ** $p < 0.01$, *** $p < 0.001$

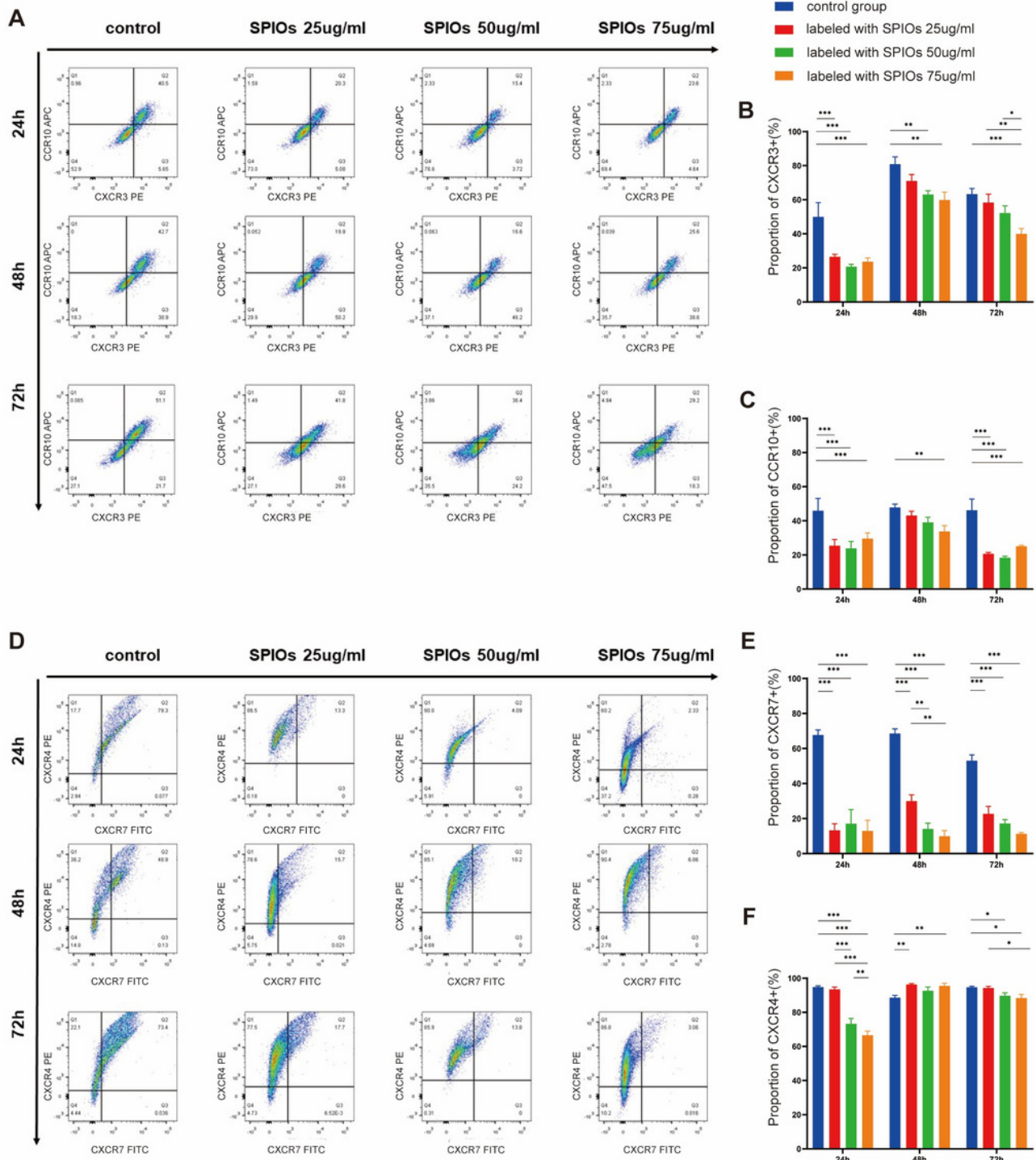


Figure 7

SPIOs labelling has no influence on the migration of BMSCs.

(A) Representative images of the BMSCs cultured in transwell chambers in the presence or absence of TAK 799, MARAVIOLIC and LY294002 with CXCL10, CCL4 or CCL19 in the lower chamber (magnification x10). (B) Migration rates in the indicated groups. Data are expressed as the mean \pm SD of each group (n=3). The colors of the bars on top right correspond to the number of migrating cells. *p<0.05, **p<0.01, ***p<0.001

